Spectroscopic and microscopic study of vanadium oxide nanotubes

Cite as: J. Appl. Phys. **101**, 084301 (2007); https://doi.org/10.1063/1.2716157
Submitted: 06 December 2006 . Accepted: 30 January 2007 . Published Online: 18 April 2007

A. Gloskovskii, S. A. Nepijko, G. Schönhense, H. A. Therese, A. Reiber, H. C. Kandpal, G. H. Fecher, C. Felser, W. Tremel, and M. Klimenkov

Spectroscopic and microscopic study of vanadium oxide nanotubes

A. Gloskovskii, S. A. Nepijko,[a] and G. Schönhense
Institut für Physik, Johannes Gutenberg-Universität Mainz, 55099 Mainz, Germany

H. A. Therese, A. Reiber, H. C. Kandpal, G. H. Fecher, C. Felser, and W. Tremel
Institut für Anorganische und Analytische Chemie, Johannes Gutenberg-Universität Mainz, 55099 Mainz, Germany

M. Klimenkov
Institut für Materialforschung I, Forschungszentrum Karlsruhe GmbH, Postfach 3640, 76021 Karlsruhe, Germany

(Received 6 December 2006; accepted 30 January 2007; published online 18 April 2007)

V_2O_5 nanotubes synthesized via the sol-gel route has been studied by electron energy loss spectroscopy (EELS), x-ray absorption spectroscopy (XAS), and energy dispersive x-ray analysis, in order to understand the local structure of vanadium in the nanotubes. Contrary to our expectation, all the features of the XAS and EELS spectra of the V_2O_5 nanotubes are in line with that of bulk layered vanadium oxide revealing that vanadium is present in the 5^+ oxidation state in the nanotubes. However, V_2O_5 nanotubes exhibit additional surface states in their electronic structure in comparison with bulk V_2O_5. A comparison of measured and calculated spectra allows us to distinguish single-wall from multiwall V_2O_5 nanotubes. © *2007 American Institute of Physics*. [DOI: 10.1063/1.2716157]

I. INTRODUCTION

Nanomaterials have received greater attention in recent years due to their superior and fascinating electronic, electrical, optical, and magnetic properties compared to their bulk counterparts. For example carbon nanotubes and fullerenes show interesting electronic and mechanical properties compared to graphite or diamond.[1] The inorganic analogs of fullerenes such as MoS_2 and WS_2 fullerenelike particles and nanotubes show superior lubricating properties as compared to 2H-MS_2 (M=W,Mo).[2–4] The magnetic susceptibility of Li intercalated $MoS_{2-x}I_y$ nanotubes is nearly three orders of magnitude higher than in Pauli metals.[5,6] However, the reasons for the extraordinary properties of these nanomaterials is largely unclear. One could speculate on many possible factors that could result in the exposition of these unusual properties, such as morphology, increase in surface area, or the surface charges or the change in the electronic structure or the quantum size.[7,8] In order to understand clearly and to selectively utilize nanomaterials for various applications, it is important to understand the local structure of the metal in these nanomaterials.

Vanadium oxide depicts an important class of transition metal oxides, where vanadium exists in various oxidation states such as V^{2+}, V^{3+}, V^{4+}, and V^{5+} in VO, V_2O_3, VO_2, and V_2O_5, respectively. Vanadium oxides and vanadium-based compounds are widely used as catalysts for hydrocarbon oxidation.[9] But many details regarding their catalytic behavior are still unclear. Vanadium oxide nanotubes have also been found to be very promising cathodes for Li-rechargeable batteries.[10,11]

Su *et al.*[12] could obtain all fine features in near edge x-ray absorption fine structure (NEXAFS) and energy loss near edge structure (ELNES) studies for a V_2O_5 single crystal using an aberration corrected Gatan spectrometer in a (scanning) transmission electron microscope. Herbert *et al.*[13] have performed band-structure calculations using WIEN97 for the various oxidation states of vanadium and the orbital hybridizations of oxygen atoms in VO, V_2O_3, VO_2, and V_2O_5. Comparative study of the simulated ELNES and the experimental electron energy loss spectroscopy (EELS) spectrum show that the major changes in the fine structures of the spectrum depend much on the changes in the O $2p$ band rather than the changes in the oxidation state of V. Bulk vanadium oxides have been subjected to many experimental and theoretical studies in the past.[14–16] Information concerning the electronic structure of vanadium oxide nanotubes is reported, for example, in Ref. 17. The electronic structure was experimentally examined by means of EELS, x-ray absorption spectroscopy (XAS), x-ray photoemission spectroscopy (XPS), and optical spectroscopy.[10,11,18,19] Magnetic properties were investigated using static magnetization and nuclear magnetic resonance.[20] In the present paper we report on surface sensitive XAS and compare it to bulk sensitive EELS studies of vanadium oxide nanotubes synthesized via sol-gel route.[21]

II. EXPERIMENT

A. Sample preparation

Vanadium oxide nanotubes were synthesized as reported in Ref. 21. An ethanolic solution of vanadium triisopropoxide and hexadecyl amine in a molar ratio of 2:1 was stirred under inert atmosphere for 1 h. The resulting yellow solution was hydrolyzed with water (5 ml/g of vanadium precursor) under vigorous stirring. The vanadium oxide composite obtained after aging (24 h) was heated in an autoclave

[a]Electronic mail: nepijko@uni-mainz.de

at 180 °C (2 days). This resulted in a black product. It was finally washed with ethanol and hexane to remove residues of unreacted amine or decomposition products and then dried at 80 °C (1 day) under vacuum.

B. Characterization

Two electron microscopy/spectroscopy techniques have been applied to characterize the obtained powder. The methods are nondestructive and are characterized by a high spatial and energy resolution.

1. Transmission electron microscopy (TEM)

The investigations were performed using a transmission electron microscope "FEI Tecnai 20 F" equipped with a Gatan image energy filter "GIF-100" for EELS measurements as well as with a high angle annular dark field (HAADF) detector. The microscope was operated at 200 kV accelerating voltage with a field emission gun; the lateral resolution was 0.14 nm. TEM images were recorded by means of a Gatan CCD camera (1024×1024 pixel^2). The EELS and energy dispersive x-ray (EDX) experiments were performed in the scanning TEM (STEM) regime using the HAADF detector with a camera length of 100 mm for particle imaging. The electron probe of 1.2 nm in diameter scans the sample surface with EELS and EDX spectra taken in each point. Experimental conditions were chosen such that the collection semiangle was 13 mrad. For EELS measurements, an energy resolution of 1.1 eV and a dispersion of 0.1 eV/channel were employed. The EDX spectra were recorded using an EDX Si/Li detector with ultrathin window.

2. X-ray absorption spectroscopy (XAS)

For comparison, we also carried out XAS measurements with higher energy resolution. They were performed at the undulator beamline U56/1-SGM at BESSY (Berlin, Germany). The XAS spectrum were obtained by the total electron yield method measuring directly the sample current while scanning the photon energy. The current was normalized to the photon intensity of the incoming beam measured via a freshly evaporated gold mesh. It is assumed that the total yield of photoelectrons is proportional to the absorption.[22] These measurements could not observe individual nanotubes but integrated over a lot of them in the photon spot on the sample. However, they are characterized by a higher energy resolution (about 75 meV in the energy range of synchrotron radiation around 500 eV). Also they allow to compare the spectra from nanotubes and bulk V_2O_5.

III. RESULTS AND DISCUSSION

A. Experimental measurements

TEM images taken in the bright field operation mode are shown in Figs. 1(a) and 1(b). As one can see, the obtained powder consists of nanotubes. The outer and inner diameters of the tubes are in the range of 100–150 nm and 20–40 nm, respectively. The tube lengths are typically several micrometers. The walls have a layered structure, i.e., they are multiwall nanotubes. Moving from the inner to the outer perimeter

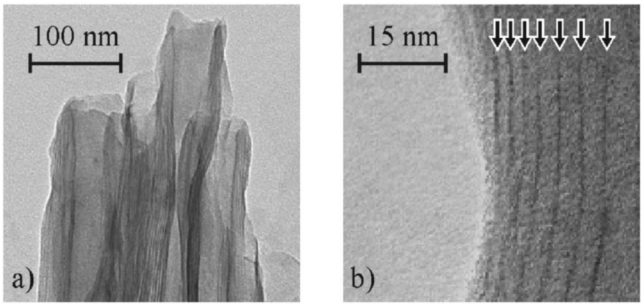

FIG. 1. (a) TEM images of multiwall vanadium oxide nanotubes. (b) Detail of a wall; arrows show the positions of the layers and their spacing varies from 4 nm in the inner region to 2.5 nm in the outer region.

of a nanotube, the distance between adjacent layer decreases from 4 to 2.5 nm and finally they become equidistant [Fig. 1(b)]. This fact can be explained by a mechanical strain in the bent layers that increases when the radius of curvature decreases.

The HAADF image is shown in Fig. 2. The walls of the nanotubes are clearly seen as bright stripes separated by a dark gap. The dark contrast of this gap testifies that there is no material in the central part of the cylindrical particles. HAADF was used due to its better sensitivity to the material atomic number z (better contrast) than in the case of the dark and bright field operation modes.

The study of the chemical composition of a separate nanotube was carried out by EDX implemented in the transmission electron microscope. For these measurements, the electron beam was focused on the sample in a region with a lateral size of 1 nm. The region, from which x-ray radiation was analyzed, was somewhat larger (it increases as the sample thickness increases, in the present case, as the nanotube wall thickness increases). The EDX analysis reveals that besides the main constituent V, Si and Cu signals are also present (Fig. 3). The Cu contribution is caused by the use of a copper grid on which there was an amorphous carbon film carrying the nanotubes. The Si signal most likely comes from Si dust located on the nanotubes. Figure 4 shows the intensity profile of the EDX signal from V $K\alpha$ radiation (area under the spectrum in the energy range from 4750 to 5150 eV in Fig. 3) along the line AB in Fig. 2. The profile of the V $K\alpha$ signal along line AB (perpendicular to the axis of the nanotube) verifies that the nanotube is a hollow cylinder. This profile is characterized by two maxima. The signal increases when the electron beam touches the

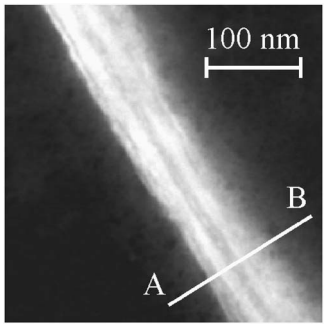

FIG. 2. HAADF image of an individual nanotube.

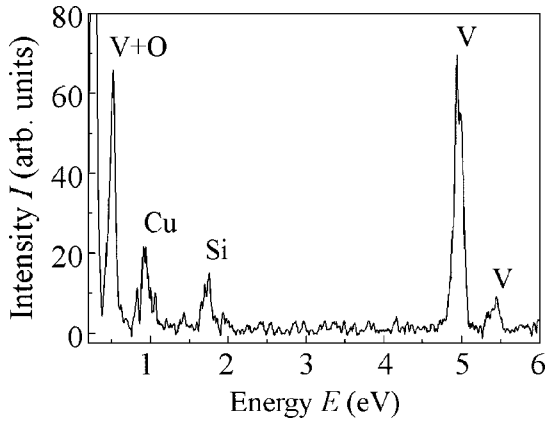

FIG. 3. EDX spectrum of an area of about 1 nm on a nanotube.

tube walls and decreases, but not to the zero level, when the electron beam is directed towards the tube axis.

In the synthesized nanotubes V should be in the oxide phase in accordance with the preparation conditions. The energy resolution of the EDX detector (125 eV in the present case) does not permit to separate the O K signal (530 eV) and the V L signal (518–530 eV).

The intensity profile of oxygen across a nanotube was measured using EELS implemented in the same electron microscope. As mentioned above, this method is characterized by a spatial and energy resolution better than 1 nm and nearly 1 eV, respectively. The curve in Fig. 5 shows the result of the EELS measurement of a selected nanotube. An experimental background has been subtracted assuming a power law. The spectrum reveals the loss peaks of V L_3 (519 eV) and L_2 (525.5 eV) as well as peaks in the range of 530–550 eV caused by the O K edge. The hatched region indicates the first peak of the oxygen near edge signal. It lies within the range of 529 eV$<E<$537 eV and is limited by the minimum of the EELS curve from above and by the EELS signal of V from below.[23] The curve in Fig. 6 shows the variation of the area of the hatched region along the line AB (denoted in Fig. 2). Thus, Fig. 6 illustrates the distribution profile for oxygen across the selected nanotube. If the integral intensity of electrons forming the peaks V L_3 and L_2 is analyzed in the same way, the distribution profile of V can

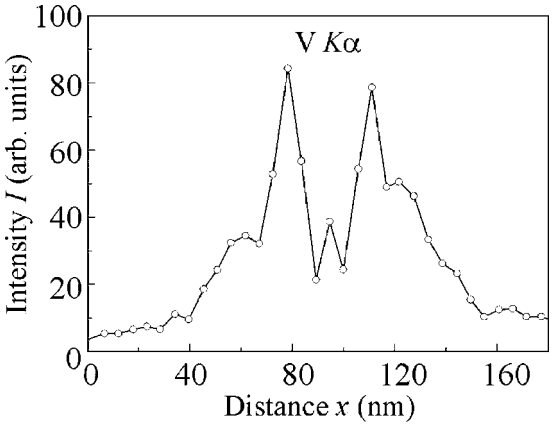

FIG. 4. Intensity line scan of the V $K\alpha$ signal (peak at 4.9 keV in Fig. 3) along the line AB drawn in Fig. 2.

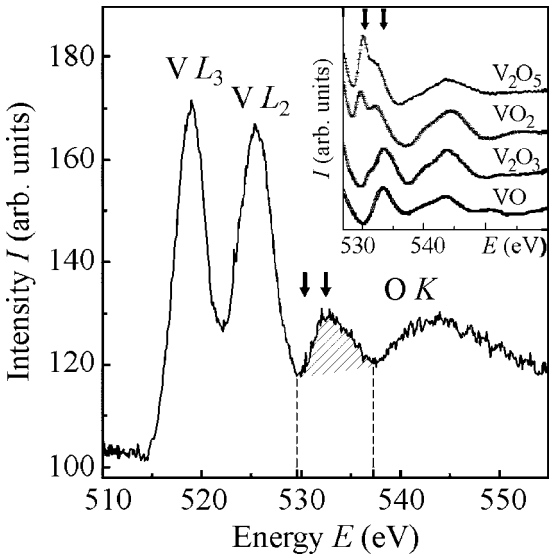

FIG. 5. Electron energy loss spectrum of a 1 nm diameter area on a nanotube. Inset: literature data for different vanadium oxide bulk samples are taken from Ref. 2. Designations (arrows, hatched area) are explained in the text.

be measured. This profile is not presented here because it reproduces very well the result of the EDX measurement given in Fig. 4. The distribution profiles for O (Fig. 6) and V (Fig. 4) coincide very closely as well. As expected, the nanotubes being studied consist of vanadium oxide.

EELS also enables to determine the type of vanadium oxide. VO, V_2O_3, VO_2, and V_2O_5 differ in the oxidation state of the V atoms: V^{2+}, V^{3+}, V^{4+}, and V^{5+}, respectively. It is caused by different coordination of the mutual arrangement of V and O atoms in the above-listed oxides. These oxides are characterized by different electronic structures and, therefore, by different densities of states (DOSs) of V and O. Differences in the shape of the V L_3 and L_2 peaks are small for different oxide phases of V, whereas the O K peak is more sensitive (compare curves in inset in Fig. 5 from Ref. 23). The maximum, at 531–534 eV has a markedly asymmetric shape (Fig. 5). Its low-energy wing has a slope larger than the high-energy wing. The energy positions of the peak components in the topmost curve of Fig. 5 (inset) are designated by arrows. They are caused by hybridization of O 2p

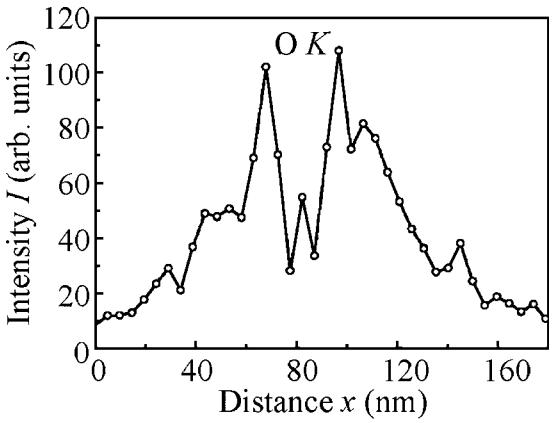

FIG. 6. Same as Fig. 4 but for the oxygen loss peak (hatched area) in Fig. 5.

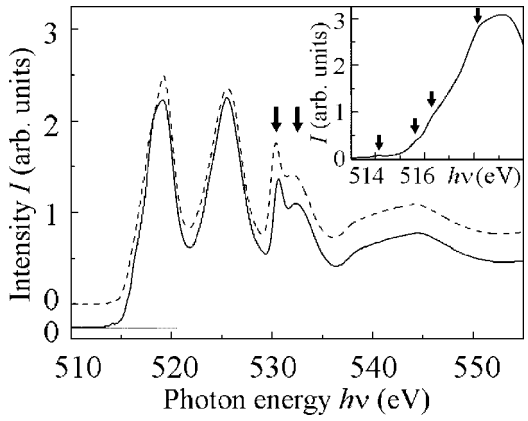

FIG. 7. X-ray absorption spectra of an ensemble of nanotubes (full curve) and a reference V_2O_5 bulk sample (dashed curve). Inset: detailed pre-edge region of the nanotubes spectrum. For details see text.

states with V 3*d* states (the latter states consist of t_{2g} and e_g orbitals).[13] The peaks at 531 and 534 eV (arrows) are caused by transitions between the 1*s* and 2*p* levels of O hybridized with the t_{2g} and e_g levels of V, respectively. The weighting t_{2g}/e_g and energy position of these peaks depend on the crystal field and are a very sensitive measure of the local surroundings of the probed atoms. For the oxide phase with maximum oxidation number V^{5+} (V_2O_5), the t_{2g} states are characterized by a higher electron density than the e_g states and determine the position of the dominating maximum at 531 eV. As the oxidation number of V decreases, the energy position of the t_{2g} and e_g levels are shifted, and the relationship between their electron densities is changed. As a result, the sum peak shifts towards higher energies (see inset in Fig. 5, from top to bottom). The same result was obtained in the band structure calculation shown in Ref. 13. Thus, the EELS measurements of different oxide phases of V are characterized by an individual shape and positions of peaks in the O *K* region. From Fig. 5 it follows that the chemical formula of the nanotube under investigation is V_2O_5. The shape and peculiarities denoted by arrows in the O *K* region of the measured spectrum and in the upper curve in the inset (from Ref. 13) are close to each other. The results found here from analysis of the shape of the spectra are in good agreement to Liu *et al.*[18] who used the energy shifts of the V $L_{2,3}$ excitation energies to determine the state of oxidation.

Figure 7 shows the results of the XAS measurements of an ensemble of nanotubes (full curve) and bulk V_2O_5 (dashed). The latter material is a semiconductor with a band gap of about 2 eV. The top of the valence band is formed by O 2*p* states and the bottom of the conduction band by V 3*d* states.[13,15,16] As expected, the XAS and EELS measurements give very similar spectra. The peaks V L_3 (519 eV) and L_2 (525.5 eV) are caused by transitions from the V 2*p* to V 3*d* levels. As these transitions are dipole allowed, the shape of the V L_3 and L_2 peaks can be interpreted by analyzing the density of unoccupied 3*d* states of V. The latter is formed by t_{2g} states in the region of 1.8–4.7 eV and e_g states in the region of 4.7–7 eV relative to the Fermi level. The density of t_{2g} states has a gap of about 0.7 eV in the region of 2.3–3 eV. Taking this into account, it is possible to interpret the features at 516.6 and 516.3 eV in the low-energy region of the V L_3 white line in spectra from nanotubes and bulk V_2O_5.

The feature at 514.1 eV manifests itself more clearly in the XAS measurements of nanotubes than for bulk V_2O_5. This agrees well with the assumption that the electronic transitions lead from V 2*p* states to surface states.[12] It is obvious that in the case of nanotubes the contribution of the surface to the integral spectrum is significantly higher than in the case of a bulk crystal. For the same reason the feature at 517.9 eV is more pronounced in the spectrum of the nanotubes.

The shape and energy positions of peaks in the spectral region O *K* in Fig. 7 also verify the oxide phase of V_2O_5. Obviously, the resolution of this spectral region in Fig. 7 is much better than that of the hatched area in Fig. 5.

Finally, the maximum at 538–550 eV in Fig. 7 (see also Fig. 5) is caused by transitions to the mixed states of O 2*p* and V 4*s* that agrees well with theoretical and experimental data.[13] This spectral region only slightly differs for different oxide phases of V; see inset in Fig. 5. In summary, the fingerprintlike x-ray absorption near edge structure (XANES) features shown in Fig. 7 unambiguously attribute the chemical state of the nanotubes to V_2O_5. Significant differences between nanotubes (full curves) and bulk V_2O_5 (dashed) reveal the higher contribution of surface states in the nanotubes than for bulk material.

B. Calculation of the electronic structure

Electronic structure calculations were performed in order to explain pecularities of the measured spectra. The limiting case of a nanotube with infinite radius is a single slab. Therefore, slab calculations were used to estimate the electronic structure of the nanotubes in comparison to bulk material. This assumption is supported by calculations in Ref. 24 showing that the DOS in various nanotubes is very similar to that of the slab. Bulk V_2O_5 exhibits already a layer-type structure and it showed up that the difference in the DOS between slabs and bulk material is also not very pronounced.

Self-consistent field (SCF) calcualtions were performed using the full potential linearized augmented plane wave (FLAPW) method based on WIEN2k.[25] The exchange correlation energy functional was parametrized within the generalized gradient approximation (GGA).[26] GGA is known to include more correlation effects compared to the pure local density approximation (LDA), which is, in particular, important for chalcogenides. The energy convergence criterion was set to 10^{-4}. For *k*-space integration, a $22\times7\times18$ mesh was used resulting in 396 irreducible *k* points for bulk calculations. For slabs, the mesh was $6\times10\times27$ with 405 irreducible *k* points in the primitive wedge of the Brillouin zone.

The space group *P mmn* (59) was assumed for the bulk calculations. The lattice parameters were set to $a=3.564$ Å, $b=11.519$ Å, and $c=4.373$ Å. This symmetry group yields one irreducible site for V atoms (Wykhoff position: 4*e*) and three sites for O atoms ($O^{1,2}$: 4*e*, O^3: 2*a*, note the superscripts here are used for numbering the atoms) such that the formula unit is V_4O_{10}. The slabs were constructed by ex-

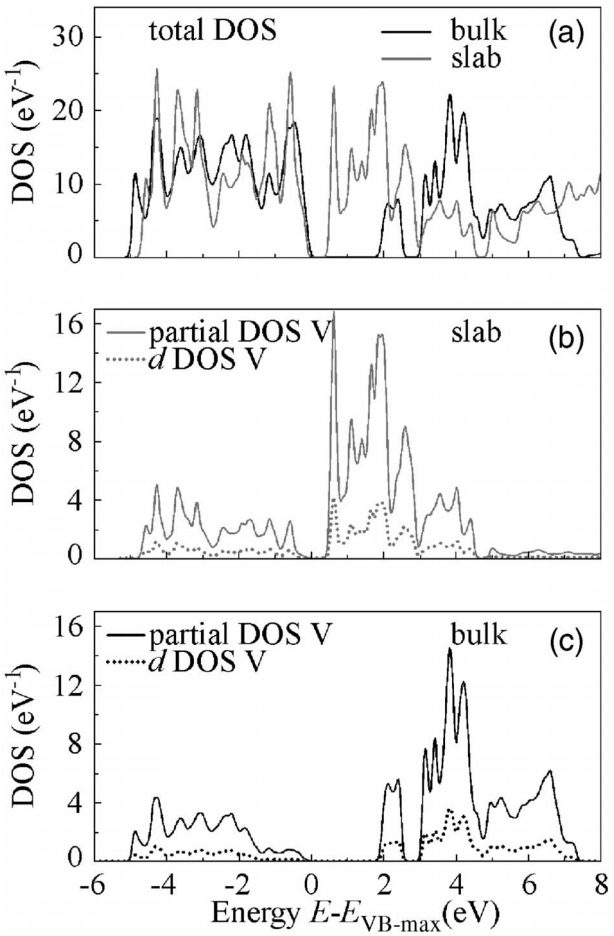

FIG. 8. Calculated DOS for V_2O_5 in bulk and slab geometries. The total DOS is compared in (a). (b) and (c) display the partial and the orbital momentum resolved DOSs at the V site. The letter is shown for the V *d* electrons.

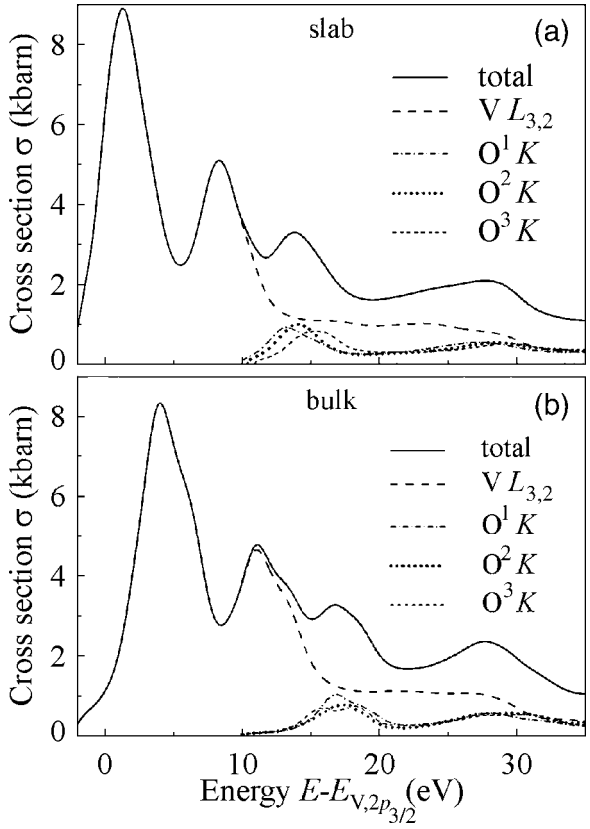

FIG. 9. Calculated x-ray absorption spectra for V_2O_5 in bulk and slab geometries. (a) shows the result for the calculation in slab geometry and (b) the result for bulk material. The spectra are decomposed into the contributions from the different atoms.

panding the *a* parameter to 18 Å resulting in the space group $P\,21/m$ providing also with one vanadium (V: 4*f*) and three oxygen ($O^{1,2}$: 4*f*, O^3: 2*e*) positions. It was carefully checked that the spacing between the layers in the *a* direction is large enough to ensure a complete decoupling of the states. The point group D_{2h} of the bulk's Γ point is reduced to C_{2h} in the slab. The V *d* states are described at the bulk's Γ point by A_g: $d_{x^2-y^2}$, d_{z^2}, B_{1g}: d_{xy}, B_{2g}: d_{xz}, and B_{3g}: d_{yz} and the O *p* states by B_{1u}: p_z, B_{2u}: p_y, and B_{3u}: p_x. The assignment of the basic wave functions to the irreducible representations in the slab is A_g: d_{xy}, $d_{x^2-y^2}$, d_{z^2} and B_g: d_{xz}, d_{yz} for the V *d* states and A_u: p_z and B_u: p_y, p_x for the O *p* states. In the real nanotubes the symmetry is reduced. In a limiting case, a nanotube is a one-dimensional object. Then it is not possible (even approximately) to distinguish between e_g and t_{2g} states as used in Ref. 13, because these irreducible representations cannot appear in the symmetry group describing V_2O_5 nanotubes. As mentioned above, even if the assignment of the electronic states is not directly possible, the DOS in large diameter tubes will be similar to the slab and in the case of multiwall tubes similar to that of the bulk.

Figure 8(a) compares the total DOS calculated for the bulk material and a slab. The principal features of the DOS, in particular, in the valence structure, are similar for bulk and slab. The bulk material turns out to be semiconducting with a gap of 1.8 eV. The conduction band of the slab, however, is shifted to lower energies, resulting in a smaller gap of only 0.4 eV. At this point the multiwall tubes may have a larger gap compared to single-wall tubes. In the latter type it may vanish completely in tubes with a small diameter. From the partial DOS [Figs. 8(b) and 8(c)], it is seen that the gap is restricted by the unoccupied states at the V site. In particular, the high density above the gap emerges from V *d* electrons. These states serve as final states in XAS from the V 2*p* initial states.

Soft x-ray absorption spectra of V_2O_5 were calculated by means of WIEN2K at the V $L_{2,3}$ and the O *K* edges. The ground state spin-orbit splitting of the V 2*p* shell was calculated to be 7.1 eV. It was used for the separation of the V white lines. The splitting between the V L_3 edge and the O *K* edge was set to the experimental value of 10 eV. The splitting of the O *K* edge for the atoms with different symmetries was set according to their 1*s* binding energies of the ground state. The intensities were mixed by scaling to the Wyckhoff site occupation.

Figure 9 displays the calculated x-ray absorption spectra for V_2O_5 in bulk and slab geometries. The slab geometry should reflect the situation in single- or double-walled nanotubes with large diameter, whereas the bulk calculation is supposed to describe better the situation in multiwall nanotubes. The calculated bulk spectra exhibit a splitting of the V $L_{2,3}$ derived intensity that is absent in the slab. The splitting

may serve to distinguish between single-walled and multi-walled nanotubes. The splitting is caused by the gap in the bulk material seen at about 2.5–3 eV above the valence band maximum in the unoccupied part of the DOS [see Fig. 8(c)]. Another splitting is only observed in the bulk calculations at the intensity from O^3 (O in the three positions). The calculated spectra are in good qualitative agreement with experimental results.

We restrict our consideration only to a qualitative agreement because the calculations were performed under a number of assumptions. In fact, it was not taken into account that the dimensional dependence of the lattice parameter manifests itself in nanotubes and changes of the lattice type can be observed. Curvature of the surface (radius of curvature is nanoscaled) results in deformation of the electron structure. At the same time, the performed calculations show which electrons form one or other peculiarities of the electron structure as well as the character of its deformation in the process of transition from single-wall to multi-wall nanotubes and further to bulk V_2O_5.

IV. CONCLUSIONS

Vanadium oxide nanotubes prepared by the sol-gel method have been investigated by TEM, EDX, EELS, and XAS. The wall thickness varied from one to a few hundred layers, the inner diameter lies in the range of 20–40 nm, and the length is typically several micrometers (it can even reach tens of micrometers). The EDX, EELS, and XAS measurements have shown that the chemical phase of the nanotubes is V_2O_5. The results are in close agreement to the recent report of Liu *et al.*[18] using XPS and EELS. Most of the measurements were performed on selected, individual nanotubes. Comparison of the XAS measurements of nanotubes and bulk V_2O_5 revealed an overall similarity but also significant differences in details between their spectra. The latter can be explained by a major contribution of surface states to the electronic structure and to electronic transitions of V_2O_5 nanotubes in comparison with the bulk material.

Distances between layers of V_2O_5 nanotubes are not equidistant if their diameters are rather small (a few tens of nanometers). When moving from the inner to the outer perimeter in such a nanotube, the distance between adjacent layers decreases and asymptotically tends to 2.5 nm.

ACKNOWLEDGMENTS

The experiments have been funded by Deutsche Forschungsgemeinschaft through Sonderforschungsbereich 625 (Teilprojekt B).

[1] M. S. Dresselhaus, G. Dresselhaus, and P. C. Eklund, *Science of Fullerenes and Carbon Nanotubes* (Academic, San Diego, CA, 1996).
[2] R. Tenne, M. Homyonfer, and Y. Feldman, Chem. Mater. **10**, 3225 (1998).
[3] L. Rapport, Yu. Bilik, M. Homyonfer, S. R. Cohen, and R. Tenne, Nature (London) **387**, 791 (1997).
[4] M. Chhowalla and G. A. J. Amaratunga, Nature (London) **407**, 164 (2000).
[5] D. Mihailovic *et al.*, Phys. Rev. Lett. **90**, 146401 (2003).
[6] Z. Jagličić *et al.*, Polyhedron **22**, 2293 (2003).
[7] S. J. Tans, M. H. Devoret, H. Dai, A. Thess, R. E. Smalley, L. J. Geerligs, and C. Dekker, Nature (London) **386**, 474 (1997).
[8] J. W. G. Wildoer, L. C. Venema, A. G. Rinzler, R. E. Smalley, and C. Dekker, Nature (London) **391**, 59 (1998).
[9] *Handbook of Heterogeneous Catalysis*, edited by G. Ertl, H. Knözinger, and J. Weitkamp (Wiley-VCH, Weinheim, 1997), Vol. 4.
[10] S. Nordlinder, A. Augustsson, T. Schmitt, J.-H. Guo, L.-C. Duda, J. Nordgren, T. Gustafsson, and K. Edström, Chem. Mater. **15**, 3227 (2003).
[11] A. Augustsson, T. Schmitt, L.-C. Duda, J. Nordgren, S. Nordlinder, K. Edström, T. Gustafsson, and J.-H. Guo, J. Appl. Phys. **94**, 5083 (2003).
[12] D. S. Su *et al.*, Micron **34**, 235 (2003).
[13] C. Herbert, M. Willinger, D. S. Su, P. Pongratz, P. Schattschneider, and R. Schlögl, Eur. Phys. J. B **28**, 407 (2002).
[14] N. Pinna, M. Willinger, K. Weiss, J. Urban, and R. Schlögel, Nano Lett. **3**, 1131 (2003).
[15] A. Chakrabarti, K. Hermann, R. Druzinic, M. Witko, F. Wagner, and M. Petersen, Phys. Rev. B **59**, 10583 (1999).
[16] V. Eyert and K.-H. Höck, Phys. Rev. B **57**, 12727 (1998).
[17] A. N. Enyashin, V. V. Ivanovskaya, Yu. N. Makurin, and A. L. Ivanovskii, Phys. Lett. A **326**, 152 (2004).
[18] X. Liu, C. Täschner, A. Leonhard, M. H. Rümmeli, T. Pichler, T. Gemming, B. Büchner, and M. Knupfer, Phys. Rev. B **72**, 115407 (2005).
[19] J. Cao, J. Choi, J. L. Musfeldt, S. Lutta, and M. S. Whittingham, Chem. Mater. **16**, 731 (2004).
[20] E. Vavilova, I. Hellmann, V. Kataev, C. Täschner, B. Büchner, and R. Klingeler, Phys. Rev. B **73**, 144417 (2006).
[21] F. Krumeich, H.-J. Muhr, M. Niederberger, F. Bieri, B. Schnyder, and R. Nesper, J. Am. Chem. Soc. **121**, 8324 (1999).
[22] W. Gudat and C. Kunz, Phys. Rev. Lett. **29**, 169 (1972).
[23] *EELS Atlas*, edited by C. C. Ahn and O. L. Krivanek (Center for Solid State Science, Arizona State University, Warrendale, 1983).
[24] V. V. Ivanosvkaya and G. Seifert, Solid State Commun. **130**, 175 (2004).
[25] P. Blaha, K. Schwarz, G. K. H. Madsen, D. Kvasnicka, and J. Luitz, WIEN2K, an augmented plane wave+local orbitals program for calculating crystal properties, Institute of Materials Chemistry, Vienna University of Technology, 2001 (see http://www.wien2k.at).
[26] J. P. Perdew, K. Burke, and M. Ernzerhof, Phys. Rev. Lett. **77**, 3865 (1996).